

INFLUENCE OF THE SHAPE OF THE IMPACTOR ON RESIDUAL STRENGTH, SIZE AND NATURE OF DAMAGE TO CFRP

WPLYW KSZTAŁTU BIJAKA NA WYTRZYMAŁOŚĆ SZCZĄTKOWĄ, WIELKOŚĆ I CHARAKTER USZKODZEŃ CFRP

Abstract

The experimental tests presented in this work concern the impact resistance test and residual strength properties after an impact performed by a drop tower INSTRON CEAST 9340. The authors prepared samples of a composite material with a polymeric matrix L285 and H285 hardener, reinforced with eight ply fabric of carbon fibre. Two shapes of the impactor (spherical and V-shape) were used to perform the testing. The samples were impacted by three values of energy (10, 15, 20 [J]). Three-point bending tests were performed to the residual strength of the samples subjected to impact tests and compared to samples which had not been damaged earlier. The study showed differences in the influence of the shapes of the impactor on the nature of the composite damage. After the test, conclusions were drawn about the influence of the shape of the impactor on the area of composite damage and its character. Also, its influence on residual strength was described. Despite the clear differences in the area of damage to composites impacted by different impactors, this does not have a significant influence on the residual strength.

Keywords: laminates, puncture resistance, impact strength, residual strength, bending strength

Streszczenie

Przedstawione w pracy badania eksperymentalne dotyczą badania udatności oraz właściwości wytrzymałości szczątkowej po uderzeniu wieżą zrzutową INSTRON CEAST 9340. Autorzy przygotowali próbki materiału kompozytowego z osnową polimerową L285 i utwardzaczem H285, wzmocnionego tkaniną ośmiowarstwową z włókna węglowego. Do badań wykorzystano dwa kształty impaktora (kulisty i V). Próbki były poddawane działaniu trzech wartości energii (10, 15, 20 [J]). Próby zginania trzypunktowego przeprowadzono do wytrzymałości szczątkowej próbek poddanych próbom udatności i porównano z próbkami, które wcześniej nie uległy uszkodzeniu. Badania wykazały różnice we wpływie kształtów impaktora na charakter uszkodzenia kompozytu. Po przeprowadzeniu badań wyciągnięto wnioski dotyczące wpływu kształtu impaktora na obszar uszkodzenia kompozytu i jego charakter. Opisano również jego wpływ na wytrzymałość resztkową. Pomimo wyraźnych różnic w obszarze uszkodzeń kompozytów pod wpływem różnych impaktorów, nie ma to istotnego wpływu na wytrzymałość szczątkową.

Słowa kluczowe: laminaty, odporność na przebicie, wytrzymałość na uderzenie, wytrzymałość resztkowa, wytrzymałość na zginanie

1. Introduction

Composite materials are now widely used in aviation structures due to their good strength-to-weight ratio and stiffness, which significantly reduces the weight of the structure compared to the materials used so far, e.g. aluminum alloys [1-4]. The most commonly used composites in the construction of

airplanes and helicopters are laminates, i.e. layered composites [5-7]. In addition, in recent years, the dynamically developing field of aviation related to UAVs began to use more and more structural materials with a small thickness [8-11]. Many composite components can be exposed to low-energy impact loads perpendicular to the component surface [12, 13].

¹ PhD. Eng. Paweł Przybyłek (corresponding author), Polish Air Force University, ul. Dywizjonu 303, 35, 08-530 Dęblin, Poland, e-mail: p.przybylek@law.mil.pl, ORCID: 0000-0002-7544-3813.

² DSc. Eng. Andrzej Komorek, Polish Air Force University, ul. Dywizjonu 303 No. 35, 08-530 Dęblin, Poland, e-mail: a.komorek@law.mil.pl, ORCID: 0000-0002-2293-714X.

³ Eng. Simone Taddeo Kaczor Di Paola, Polish Air Force University, ul. Dywizjonu 303 No. 35, 08-530 Dęblin, Poland, e-mail: s.kaczordipaola4754@wsosp.edu.pl

⁴ Eng. Łukasz Komorek (corresponding author), Polish Air Force University, ul. Dywizjonu 303 No. 35, 08-530 Dęblin, Poland, e-mail: l.komorek5374@wsosp.edu.pl

This type of load is especially common in the maintenance process of aircraft [14-16] and despite the low energy value, they often result in deterioration of the strength properties of the composite element [17-21]. There are numerous conditions for this impact: hailstones and bird strikes being the most significant ones, owing to their high chance of occurrence [22-25]. On the other hand, a tyre piece can strike the wing structures and the ice coming from the propeller blade edge could also impact the nacelle of the aircraft engine [26]. Therefore, the study of impact behaviors and residual strength of CFRP laminates is necessary to improve the impact resistance and damage tolerance of the composite. The damage evaluation criteria (including dent depth, DDPA (delamination damage projection area), energy dissipation, RBS (residual bending strength), etc.) are vital for the assessment of the damage status of laminates [17-21]. Due to the damage caused by the action of transverse impact loads, the following can be distinguished:

- BVID – barely visible impact damage,
- VID – visible impact damage.

BVID defined by two aircraft manufacturers, Airbus and Boeing, is damage caused by an impact and it is determined only by the depth and area of the damage, which cannot be detected during inspection, visual inspection under typical lighting conditions from a distance of 1.5 m [28]. There are many studies in the literature that determine the influence of various factors on puncture resistance, damage tolerance or other strength parameters [22]. They are analyzed and checked experimentally in order to find the best solutions. The basic factors are the architecture of the fabric and the properties of the matrix, which have the most significant influence on the puncture resistance of composites reinforced with fiber. The secondary factors include: fiber hybridization, matrix hybridization, hygrothermic factors, the sequence of layering, impactor geometry (mass, size, shape), impact repeatability [29]. The constituent and geometrical parameters are broadly investigated parameters in the study of impact mechanics of composites. Relatively little interest has been given in the literature to the impactor shape, size, velocity, mass, and angle and this effect is still not entirely formulated. [30-34]. The influence of the impactor in specific, the combined effects of impactor nose shape, the angle of obliquity, mass, size and boundary condition on the impact resistance of composite materials are not clearly addressed [22]. Due to the very wide use of such materials for the construction of aircraft covers, tests were carried out on the resistance of composites to low-energy impact loads to which composite structures of aircraft are exposed during everyday operation. This is a very important feature due to the fact that at low energy

values (1... 3 J) no signs of material destruction are visible from the side of load application. This is evidenced by the amount of research conducted in the last two decades, eg. in [35] the authors presented historical developments in the study of composite structures under high velocity impact events by analyzing 27 works on this subject in various terms. Moreover, as previously mentioned, despite the many studies carried out on the influence of the shape, mass and size of the "impactor" on the impact resistance, this effect is still not clearly formulated. For many reasons (including economic), visual inspection remains the most popular method of locating impact damage of aircraft structure and it has been included in relevant normative documents for many years [36,37]. Visual inspection is relatively fast as a primary method and has a large field of view for the in-service inspection of composite structures. Therefore, visual inspection is also one of the important basis for defining Barely Visible Impact Damage (BVID). Therefore, it is necessary to determine the correlation between the size of the damage and the decrease in strength properties in order to unequivocally carry out the damage assessment, which will allow to make a decision on the efficiency of the aircraft. This article presents the results of tests of the puncture resistance of CFRP subjected to a three-energy (10, 15, 20 [J]) impact and two-shape impactors. As a comparative parameter, the damage surface areas of the laminate from the impact side and the opposite side were adopted, and the peak values of force, energy and displacement were taken into account (Peak force [N], Peak Energy [J], Peak displacement [mm]) and relative properties: Peak force on thickness [kN/m], Peak energy on thickness [J/m]. Moreover, in order to analyze and evaluate the influence of the shape of the "impactor" and the impact energy on the strength properties of the tested composite, the bending strength and bending modulus of the previously impacted specimens were determined.

2. Experimental investigation

2.1. Preparation of samples for testing

A symmetric cross-ply laminate was made using the hand lamination method. It was then placed in a Mecamac hydraulic press for 24 hours under a pressure of 1 [MPa].

The composite matrix is a certified aerospace epoxy resin, L285, cross-linked with H285 hardener (Table 1).

The reinforcement was a carbon-fibre fabric designated GG-416 T and produced by G. ANGELONI with a twill weave (diagonal) and the parameters shown in Table 2.

Table 1. Parameters of resin L285 and hardener H285

List of mechanical parameters for LG285 resin		
Parameter	Unit	Value
Bending strength	MPa	110 – 120
Modulus of elasticity in bending	MPa	2,700 – 3,300
Tensile strength Rm	MPa	75 – 85
Compressive strength	MPa	130 – 150
Elongation	%	5 – 6.5
Fatigue strength	KJ/m-2	38 – 48
Shore hardness	-	85

Table 2. Parameters of reinforcement fabric

Symbol	Weight (g/m ²)	Weave
GG 416 T	416	Dual 2 2/ 2
	Fibre/Bundle	
	Matrix	Matrix
	carbon 800 tex	carbon 800 tex
	Thickness (mm)	
	0.41	

Thirty-four 60x80mm rectangular samples were prepared from the composite. They were grouped into seven batches.

2.2. Impact resistance tests

The impact resistance tests were conducted on an INSTRON CEAST 9340 drop tower. The samples were subjected to transverse impact loads of 10, 15, and 20 J energies. Two "impactors" were used, the first one with a spherical shape, 20 mm in diameter, and the second one wedge-shaped (V-shaped) with an opening angle of 30° and a striking edge radius of 3 mm (Fig. 1). A series of at least 3 samples was made for each energy and each impactor. The samples were placed on the stage without fixing.



Fig. 1. Shapes of 'impactors' used in the tests

The examination parameters for specific energies have been presented in Table 3.

A number of parameters were obtained as a result of the research. The parameters were later used to analyse the impact resistance in the aspect of the 'impactor' shape. Damage to the composites was caused as a result of the impact on the test material,

which was assessed. The damage areas of the laminate on the impacted side and the opposite side were used as a comparative parameter. The selected and representative images along with marked areas of damage, after an impact, with different energies and impactors are presented in Figure 2 and Figure 3.

Table 3. parameters of impact resistance test

Impact energy [J]	Weight [kg]	Height of the impactor [mm]	Impact speed [m/s]
10	2.65	385.0	2.72
15		577.0	3.33
20		770.0	3.85

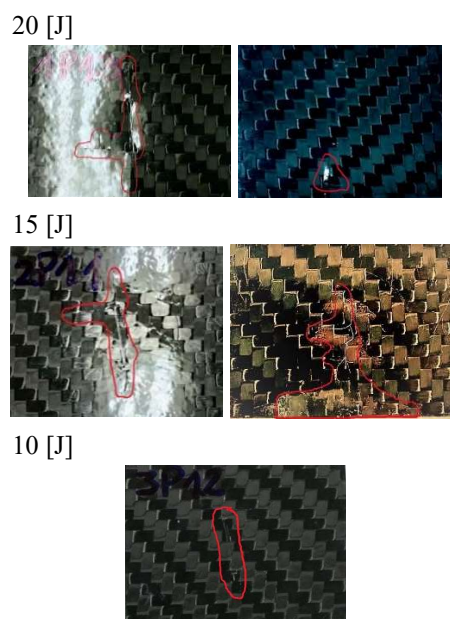


Fig. 2. Damage area of a sample impacted by a wedge-shaped impactor from the impacted side and opposite side

In the case of samples struck with a wedge 'impactor' on the impacted side, the composite was damaged with a shape reflecting that of the impactor (Fig. 2). Depending on the energy of the impact, there was cracking of the reinforcement along the fibres of the fabric with a different depth and area. For an impact energy of 10 [J], the damage on the impacted side is tiny, with an average area of approximately 150 mm². Furthermore, no damage to the laminate was observed on the side opposite to the impacted side.

The surface of the samples impacted by the spherical impactor caused damage in the form of an indentation, which initiated cracks in the horizontal and vertical cross-shaped reinforcement fabric (Fig. 3). Similarly to the previous 'impactor', the area of damage depends on the energy of the impact. Damage was observed on the surface opposite to the impacted area for each energy. For the highest energy value (20 [J]) there is also a clear perforation of the laminate.

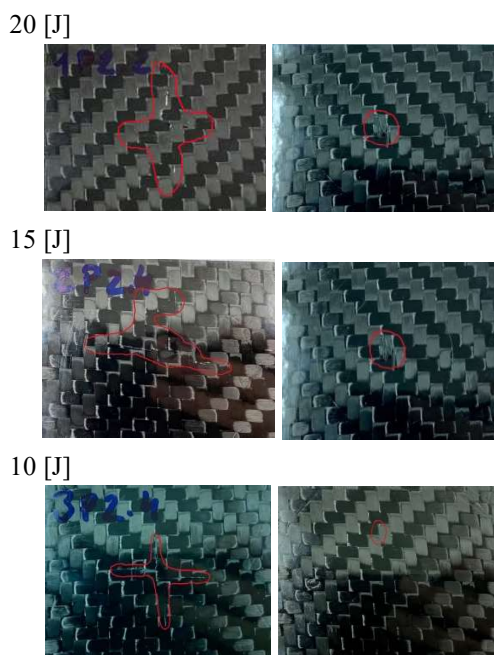


Fig. 3. Damage area of a sample struck by a spherical shaped impactor from the impacted side and opposite side.

When comparing the damage areas on the impacted side (Fig. 4) and on the opposite surface (Fig. 5), some regularities can be noticed in the aspect of the shape of the "impactor."

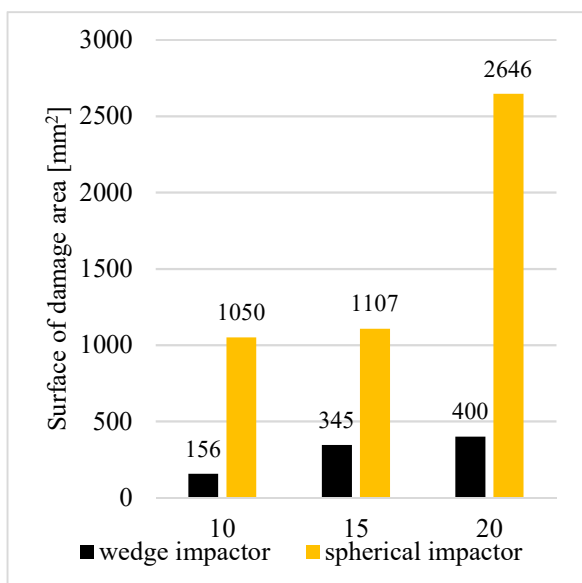


Fig. 4. Damage area on the impacted side

The damage area of the tested composite is always larger for a spherical 'impactor'. The damage to the samples is approximately 6.5 times greater with a spherical 'impactor' on the struck surface (Fig. 4). However, on the surface opposite to the impacted surface (Fig. 5), the damage is comparable and only approximately 10 % larger for the spherical impactor. On both the impacted and counter-impacted surfaces,

the difference in damage size for both impactors depends on the impact energy. The largest damage area was recognized after impact with 20 [J] energy, but especially in the counter-impacted surface difference for wedge impactor is about 30% and about 80% for spherical impactor.

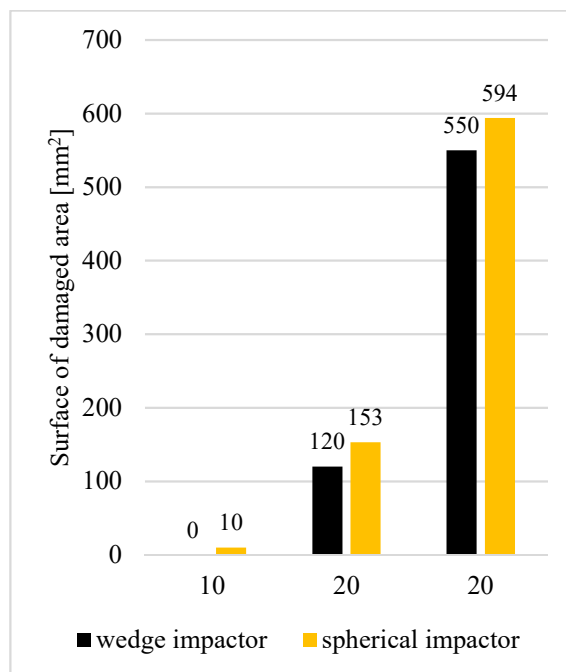


Fig. 5. Surface area of damage on the opposite side from the impacted side

Other recorded parameters were also taken into account for a more detailed analysis of puncture resistance. Peak force, energy and deformation (peak force [N], peak energy [J], peak displacement [mm]) and relative properties were considered to assess puncture resistance: peak force on thickness [kN/m], peak energy on thickness [J/m]. The dropping hammer is equipped with a force sensor; based on its value, the energy (1), (2), and deformation (3) are calculated according formulas presented below.

$$E_i = \int_i F(\varepsilon) \quad (1)$$

$$E_i = \sum_{i=0}^{i-1} E_i + t_{\text{sampling}} \frac{F_i v_i + F_{i-1} v_{i-1}}{2} \quad (2)$$

$$\varepsilon_i = \sum_{i=0}^{i-1} \varepsilon_i + t_{\text{sampling}} \frac{v_i + v_{i-1}}{2} \quad (3)$$

where: t_{sampling} – sampling time,
 v – rate of change of strain,
 F – measured force.

The results, which were used to analyse the puncture resistance of the tested material in terms of the 'impactor' shape are presented in Table 4.

Table 4. Results of the examination: impact resistance

Impact energy [J]	Peak Force [N]	Peak Energy [J]	Peak Displacement [mm]	Peak force on thickness [kN/m]	Peak energy on thickness [J/m]
"Wedge impactor"					
10	7,234.93	9.68	2.31	3,448.28	6,649.17
15	8,556.96	14.22	3.16	2,966.24	4,985.07
20	9,956.87	19.19	3.57	2,527.13	3,439.11
"Spherical impactor"					
10	6,723.84	9.59	2.83	2,241.28	3,197.02
15	8,379.74	14.58	3.78	2,912.90	5,073.39
20	9,006.27	17.08	4.07	3,175.00	6,201.11

Based on the obtained parameters, it can be concluded that the force transmitted by the test material mainly depends on the value of the impact energy and is highest for the highest impact energies. It only slightly depends on the shape of the "impactor". The differences in peak force values (Peak Force) are only about 10 % and increase with the impact energy. In order to analyse the puncture resistance in detail, a comparison was also made of the force variation (Fig. 6, Fig. 7) over time and the force variation with respect to deformation (Fig. 8, Fig. 9).

By comparing the characteristics of force variation over time, it is possible to see significant differences in the behaviour of the examined material when impacted with different 'hammers'. In the case of a 'spherical impactor', the change in impact energy does not affect the way the composite responds to the impact; also the shape of the curve indicates its elastic nature.

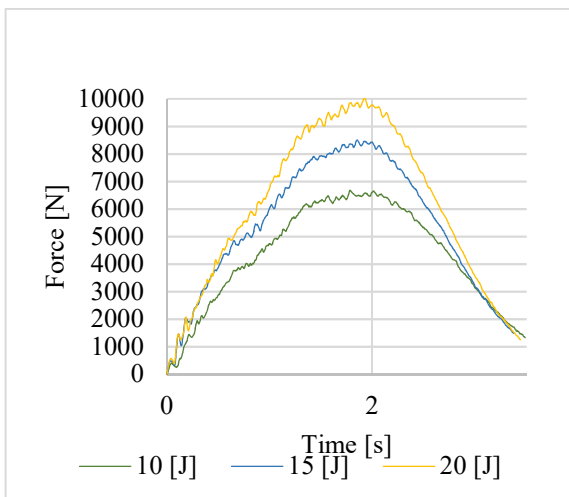


Fig. 6. Force variation during in impact with a spherical "impactor"

In addition, the response (contact) time of the composite is identical for all impact energies. In the case of a 'wedge hammer', the nature of the curve

(Force-Time) (Fig. 7) indicates permanent deformation under impact loading and damage within the composite.

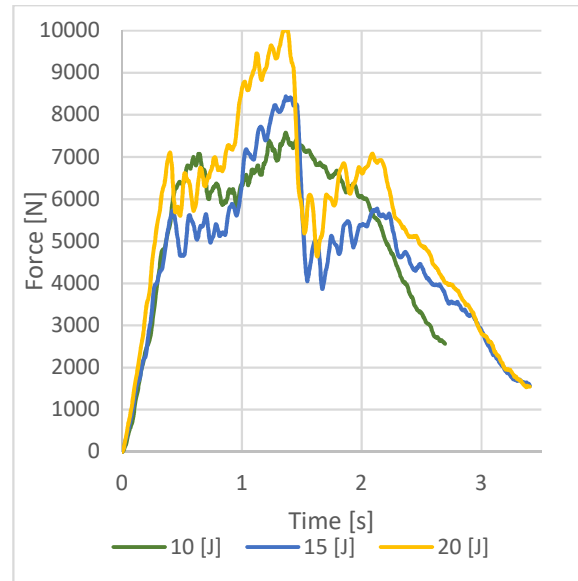


Fig. 7. Force variation curves during an impact with a wedge-shaped impactor

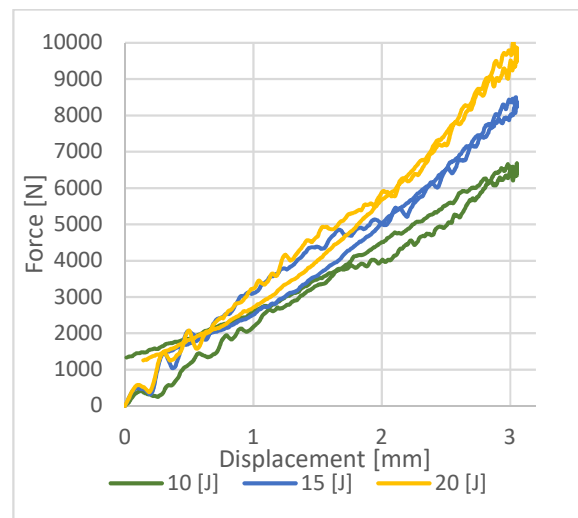


Fig. 8. Force-deformation curves for the impact of a spherical "impactor"

Furthermore, the nature of the composite response for an impact energy of 10 [J] is different for all impact energies, the force at which the destruction process of the F_{ini} composite is initiated. It is similar and it can be assumed that this is the value of the load at which the impact layer of the composite perforates and thus breaks the fibres of the reinforcement. An oscillation of force values can then be observed, which are indicative of specific 'stress waves' in the material and damage to the matrix 'layer' occurring in-between the reinforcement layers. The force then builds up until it reaches its maximum value of F_{max} (Peak Force). The

rapid decrease in its value, after F_{max} has been reached, indicates deceleration of the damage process and the true puncture resistance of the test material. For the impact energies of 15 and 20 [J], a repeat increase in force can be observed until another specific extreme is reached, which indicates the response of the next reinforcement layer to the load. On the basis of these changes, it can be estimated that the "wedge hammer" caused internal damage to the laminate and that its depth along the thickness of the test material depends on the impact energy.

The characteristics of the change in force versus deformation (Fig. 8, Fig. 9) allow the energy absorbed by the laminate to be estimated (area inside the curve-area under the force-deflection curve).

The slope of the curve provides an estimate of the stiffness of the composite and the shape of the curve indicates the nature of the damage to the composite. In the case of tests carried out with two different shape impactors, there was no complete perforation of the composite, as evidenced by the closed loop of the curve and the return of the force with respect to deformation at the initial value. However, there is clearly a change in the nature of the composite's response to an impact depending on the shape of the 'impactor'. Also, the value of the absorbed energy depends on the type of used 'impactor'.

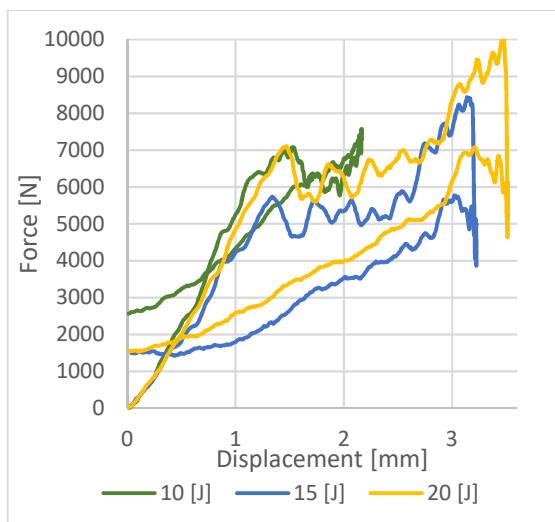


Fig. 9. Force vs. deformation curves for a wedge-shaped impactor

Furthermore, in the case of the 'wedge impactor', the amount of absorbed energy depends on the value of the impact energy, as indicated by the changes in the shape of the force-deformation characteristics (Fig. 9).

2.3. Bending flexular strength test

In the next stage of experimental testing, the samples previously subjected to transverse impact

loads (impact) were tested to determine the residual strength, i.e. the bending strength.

The test was conducted in a three-point bending scheme on a ZWICK/ROELL Z5 testing machine in accordance with PN EN ISO 178, at the support span of $L=46$ mm (Fig. 10).

As a result of the study, the following were determined:

- σ_{FM} – bending strength [MPa],
- E_f – modulus of elasticity in bending [GPa].



Fig. 10. Bending flexural strength test

The obtained results were related to the control (non-impacted) samples and the results are presented in Figures 11, 12, 13.

The changes in the bending strength values are mainly dependent on the impact energy and, compared to the control samples (not subjected to an impact), there was a decrease of approximately 40% for an impact energy of 10 [J], 50% for an impact energy of 15 [J] and 60% for an impact energy of 20 [J].

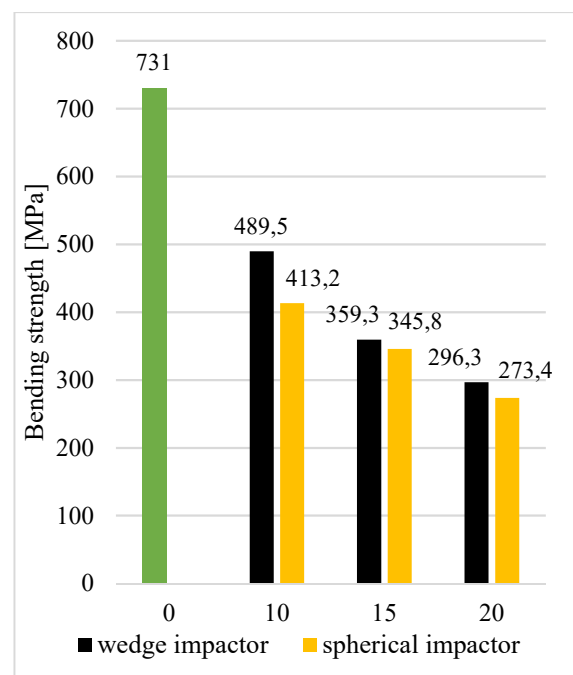


Fig. 11. Bending strength σ_{FM} [MPa]

In all the cases, the "wedge impactor" resulted in a greater decrease in bending values strength. However, depending on the shape of the "impactor", the differences are negligible: approximately 10% for an energy of 10 [J], approximately 3% for an impact energy of 15 [J] and 20 [J]. In the case of changes in the modulus of elasticity in bending, the 'spherical impactor' caused its even larger decline: 35% for an impact energy of 10 [J], 50% for an impact energy of 15 [J] and 60% for an impact energy of 20 [J].

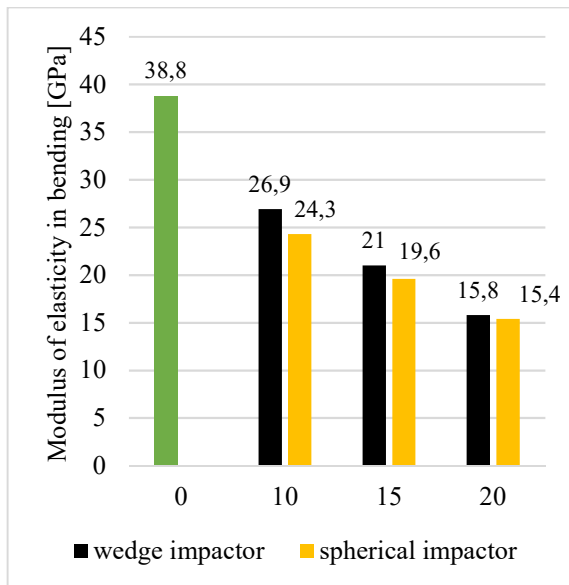


Fig. 12. Modulus of elasticity in bending E_r [GPa]

The differences with regard to the 'impactor' shape are minimal and decrease along with an increase in an impact energy: approximately 5% for an impact energy of 10 [J], approximately 3% for an impact energy of 15 [J] and 1% for an impact energy of 20 [J].

3. Conclusions

The conducted puncture resistance tests made it possible to estimate the effect of impacts with two 'impactor' shapes and three energies (10, 15, 20 [J]) on both the extent and nature of damage to the layered composite with a carbon fibre reinforcement and on the degradation of the strength properties: bending strength σ_M and the modulus of elasticity in bending E_r . It also made it possible to formulate conclusions.

The shape of the impactor influences the magnitude of the analysed parameters, such as damage area or strength parameters, declining along with an increasing impact energy;

The damage area of the tested composite is always larger for the spherical 'impactor'. However, on the surface opposite to the impacted surface damage, the damage is comparable and is only approximately 10% larger for the spherical impactor.

The "wedge impactor" resulted in a greater decrease in bending strength. However, the variation in its value mainly depends on the impact energy; the differences in the aspect of the 'impactor' shape decrease with an increasing impact energy, amounting to approximately 10% for the impact energy 10 [J], approximately 3% for the impact energy 15 and 20 [J].

Detailed comparisons of the force variation curves (Fig. 6, Fig. 7) over time and of the force variation with respect to deformation makes it possible to conclude that the "wedge impactor" caused internal damage to the laminate and that its "depth along the thickness of the examined material depends on the impact energy.

References

1. Soutis Constantine. 2005. Fibre reinforced composites in aircraft construction. Progress in Aerospace Sciences. Volume 41, Issue 2, 143-151, doi.org/10.1016/j.paerosci.2005.02.004.
2. A.J. Beck, A. Hodzic, C. Soutis, C.W. Wilson, 2009. IOP Conf. Ser.: Mater. Sci. Eng.
3. Y.X. Zhang, Zhi Zhu, Richardson Joseph, Isfakul Jamal Shihan. 2020. Damage to aircraft composite structures caused by directed energy system: a literature review. Defence technology. <https://doi.org/10.1016/j.dt.2020.08.008>.
4. Fengyang Jiang, Zhidong Guan, Zengshan Li, Xiaodong Wang. 2021. A method of predicting visual detectability of low-velocity impact damage in composite structures based on logistic regression model. Chinese Journal of Aeronautics. 34(1): 296-308.
5. Królikowski Waclaw 2012, Polimerowe kompozyty konstrukcyjne. Warszawa, Wydawnictwo Naukowe PWN.
6. Bruno Castanie, Christophe Bouvet, Malo Ginot. 2020. Review of composite sandwich structure in aeronautic applications, Composites Part C: Open Access 1.
7. Xianfeng Yang, Jingxuan Ma, Dongsheng Wen, Jialing Yang. 2020. Crashworthy design and energy absorption mechanisms for helicopter structures: A systematic literature review, Progress in Aerospace Sciences 114.
8. Qi Liu, Zhangzhi Ge, Wei Song. 2016. Research Based on Patent Analysis about the Present Status and Development Trends of Unmanned Aerial Vehicle in China, Open Journal of Social Sciences, Vol. 4, No. 7.
9. Daeil Jo, Yongjin Kwon. 2017. Development of Rescue Material Transport UAV (Unmanned Aerial Vehicle), World Journal of Engineering and Technology, Vol. 5, No. 4.
10. Jiawen Yu. 2018. Design and Optimization of Wing Structure for a Fixed-Wing Unmanned Aerial Vehicle (UAV), Modern Mechanical Engineering, Vol. 8, No. 4.
11. Mohamed M. ElFaham, Ayman M. Mostafa, G.M. Nasr. 2020. Unmanned aerial vehicle (UAV) manufacturing materials: Synthesis, spectroscopic characterization and dynamic mechanical analysis (DMA), Journal of Molecular Structure 1201. <https://doi.org/10.1016/j.molstruc.2019.127211>.
12. R.C. Batra, G. Gopinath, J.Q. Zheng. 2012. Damage and failure in low energy impact of fiber-reinforced polymeric

- composite laminates, *Composite Structures*, Volume 94, Issue 2. 540-547. <https://doi.org/10.1016/j.compstruct.2011.08.015>.
13. G. Perillo, J.K. Jørgensen. 2016. Numerical/Experimental Study of the Impact and Compression after Impact on GFRP Composite for Wind/Marine Applications, *Procedia Engineering*, Volume 167. 129-137, <https://doi.org/10.1016/j.proeng.2016.11.679>.
 14. Ravi B. Gondaliya. 2016. Improving Damage Tolerance of Composite Sandwich Structures Subjected to Low Velocity Impact Loading: Experimental and Numerical Analysis, *Dissertations and Theses*, Embry-Riddle Aeronautical University Daytona Beach.
 15. Ercan Sevkat, Benjamin Liaw, Feridun Delale, Basavaraju B. Raju. 2009. Drop-weight impact of plain-woven hybrid glass-graphite/toughened epoxy composites, *Composites: Part A* 40. 1090–1110.
 16. U.S. Department of Transportation, Federal Aviation Administration, 'Composite aircraft structure', Advisory Circular AC No: 20-107B, Change 1, 24 August 2010.
 17. Qihui Lyu, Ben Wang, Zhenqiang Zhao, Zaoyang Guo. 2022. Damage and failure analysis of hybrid laminates with different ply-stacking sequences under low-velocity impact and post-impact compression, *Thin-Walled Structures* 180.
 18. Mubarak Ali, S.C. Joshi, and Mohamed Thariq Hameed Sultan, 2017. Palliatives for Low Velocity Impact Damage in Composite Laminates, *Advances in Materials Science and Engineering*, 16 pages. <https://doi.org/10.1155/2017/8761479>.
 19. Ramesh Talreja, Nam Phanb. 2019. Assessment of damage tolerance approaches for composite aircraft with focus on barely visible impact damage, *Composite Structures* 219. 1–7.
 20. Botelho E.C., Silva R.A., Pardini L.C., Rezende M.C. 2006. A review on the development and properties of continuous fiber/epoxy/aluminum hybrid composites for aircraft structures. *Materials Research*. 9(3): 247–256. doi: 10.1590/S1516-14392006000300002.
 21. Komorek A., Przybyłek P. 2012. Examination of the influence of cross-impact load on bend strength properties of composite materials, used in aviation. *Eksploatacja i Niezawodność*. 14, 265-269.
 22. J. Jefferson Andrew, Sivakumar M. Srinivasan, A. Arockiarajan, Hom Nath Dhakal, 2019. Parameters influencing the impact response of fiber-reinforced polymer matrix composite materials: A critical review, *Composite Structures* 224.
 23. Airoidi A., Cacchione B. 2006. Modelling of impact forces and pressures in Lagrangian bird strike analyses. *Int J Impact Eng* 32:1651–77.
 24. Anghileri M., Castelletti L.M.L., Invernizzi F., Mascheroni M. 2005. A survey of numerical models for hail impact analysis using explicit finite element codes. *Int J Impact Eng* 31:929–44.
 25. Stanislav Dubinskii, Vitaliy Senik, Yuri Feygenbaum, 2019. The Significance of In-Service Factors for the Visual Detectability of Impact Damage in Composite Airframe, *Journal of Nondestructive Evaluation*. 38:91 <https://doi.org/10.1007/s10921-019-0632-3>.
 26. M. Drożdźziel, P. Jakubczak, J. Bieniaś. 2021. Low-velocity impact resistance of thin-ply in comparison with conventional aluminium-carbon laminates, *Composite Structures*, Volume 256.
 27. Jianwu Zhoua, Binbin Liaob, Yaoyao Shia, Yangjie Zuoc, Hongliang Tuod, Liyong Jiae, 2019. Low-velocity impact behavior and bending tensile strength of CFRP Laminates, *Composites Part B* 161. 300–313.
 28. S.N.A. Safri, M.T.H. Sultan, N. Yidris, F. Mustapha, 2014. Low Velocity and High Velocity Impact Test on Composite Materials – A review, *The International Journal Of Engineering And Science*, Volume 3, Issue 9, 50-60.
 29. S. Shah, S. Karuppanan, P. Megat-Yusoff i Z. Sajid, 2019. Impact resistance and damage tolerance of fiber reinforced composites: A review. *Composite Structures*, tom 217. 100-121.
 30. Mitrevski T., Marshall I.H., Thomson R., Jones R. 2006. The influence of impactor shape on the damage to the composite laminates. *Compos Struct*. 76:116–22.
 31. Zhou G., Lloyd J.C., McGuirk J.J. 2001. Experimental evaluation of geometric factors affecting damage mechanisms in carbon/epoxy plates. *Composites Part A*. 32:71–84.
 32. Dhakal H.N., Zhang Z.Y., Bennett N., Reis P.N.B. 2012. Low-velocity impact response of non-woven hemp fibre reinforced unsaturated polyester composites: Influence of impactor geometry and impact velocity. *Compos Struct*. 94:2756–63.
 33. Zarei Hamed, Sadighi Mojtaba, Minak Giangiacomo. 2017. Ballistic analysis of fiber metal laminates impacted by flat and conical impactors. *Compos Struct* ;161:65–72. ISSN 0263-8223.
 34. Artero-Guerrero J.A., Pernas-Sánchez J., López-Puente J., Varas D. 2015. Experimental study of the impactor mass effect on the low velocity impact of carbon/epoxy woven laminates. *Compos Struct*. 133:774–81. ISSN 0263-8223.
 35. N. Razali, M.T.H. Sultan, F. Mustapha, N. Yidris, M.R. Ishak. 2014. Impact Damage on Composite Structures – A Review, *The International Journal Of Engineering And Science (IJES)*. Volume 3. Issue 7. 08-20.
 36. FAA. Advisory circular composite aircraft structure. Washington D.C.: Federal Aviation Administration; 2009. Report No.: 20–107 (B); . SAE International. CMH-17 Composite Materials Handbook volume 3. polymer matrix composites materials usage, design, and analysis. Warrendale: SAE. International 2012.
 37. Spencer F.W. 1996. Visual inspection research project report on benchmark inspections. Washington D.C.: Federal Aviation Administration. Report No: DOT/FAA/AR-96/6.